Available online at www.sciencedirect.com
ScienceDirect
Journal of the European Ceramic Society 27 (2007) 1143–1149
www.elsevier.com/locate/jeurceramsoc

Effect of bonding layer on the electromechanical response of the cymbal metal-ceramic piezocomposite

P. Ochoa [a,*], J.L. Pons [b], M. Villegas [a], J.F. Fernandez [a]

[a] *Electroceramic Department, Instituto de Cerámica y Vidrio, CSIC, c/Kelsen 5, 24049 Madrid, Spain*
[b] *Instituto de Automática Industrial, CSIC, 28500 Arganda del Rey, Madrid, Spain*

Available online 27 June 2006

Abstract

In the present work finite element analysis, FEA, ATILA® models were generated to analyse the frequency behaviour of cymbals as a function of the bonding layer. The experimental frequency responses were correlated with predicted values. The epoxy thickness variation, the presence of epoxy meniscus or lacks of adhesive contribute to the frequency dispersion of the vibration modes.

A statistical rupture test was developed where the cymbals were axially loaded in a universal mechanical test machine and monitored with an electrometer. The debonding was revealed by the generated charge versus the applied force. The adequate relationships between bonding nature, frequency response and debonding were established and shown that the asymmetries are the main parameter to control in the cymbal assembly.

Keywords: Composites; Failure analysis; Piezoelectric properties; PZT; Finite element analysis

1. Introduction

The cymbal design has demonstrated higher displacement, effective piezoelectric coefficient, temperature stability, generative force and charge amplification than previous design.[1,2] In addition it is able to obtain low acoustic impedance, mass reduction and high sensitivity to weak hydrostatic waves.

The cymbal design consists of a piezoelectric ceramic disk sandwiched between two truncated conical metal endcaps using epoxy as a bonding agent. The metal endcaps serve as mechanical transformers to convert and amplify the radial motion of the ceramic disk into a large axial displacement normal to the endcaps. Both the d_{31} (=d_{32} for disk) and the d_{33} coefficient of the ceramic contribute to the axial displacement of the composite, resulting in a very high effective d_{33} value. Advantages of the cymbal transducers are the easiness of tailoring the desired properties[2] by the choice of the cap and driver materials, together with the geometry and overall dimensions, with cost effective manufacturing, thereby accommodating this design to numerous applications. Due to the reversibility of the piezoelectric effect, cymbals, like the other piezoelectric devices, can be exploited both as sensor and actuators. Then, potential applications of the cymbal transducer are compact and inexpensive hydrophones, fish finders, towed undersea arrays, underwater imaging, geophysical research, actuators and smart system for active vibration control.

If the cymbal device is compared with other of the most relevant and well established emerging actuators, like magnetostrictive actuators,[3] advantages of the cymbals are bigger relatives forces (several orders of magnitude), mainly due to the accompanying components required to set up bias magnetic fields or to pre-stress the magnetostrictive actuator, then, smaller dimension, and bigger resonance frequency than magnetostrictive actuators, this is closely related to the lower Young's modulus of magnetostrictive actuators and the limits due to eddy currents.

Up to now, studies of the cymbal piezocomposite are focussed on the impedance frequency response and their characterization as underwater transducer and sound emitters.[4,5] However, their functional behaviour and reliability have never been discussed and studied. Therefore, it is needed a electromechanical characterization that allows us to know how this ceramic-metal composite reacts when a external mechanical force it's applied.

* Corresponding author at: Instituto de Cerámica y Vidrio (CSIC), c/Kelsen 5, Cantoblanco, 24049 Madrid, Spain. Tel.: +34 91 735 58 40; fax: +34 91 735 58 43.
E-mail address: ochoa@icv.csic.es (P. Ochoa).

0955-2219/$ – see front matter © 2006 Elsevier Ltd. All rights reserved.
doi:10.1016/j.jeurceramsoc.2006.05.022

2. Description of experimental set-up and method

The piezoelectric ceramics used to build up the composite transducers were piezoceramic disks type PZT-5A.[6] Kovar alloy was chosen as the metal endcap material because its thermal expansion coefficient is quite similar to the PZT one and, thus, the thermally induced displacement (TID) is reduced.[2] In a first step metal disks with a diameter of 12.7 mm were punched from 0.25 mm thick Kovar sheets. In a second step the metal disks were shaped using specially shaped dies by uniaxial pressing at 74 MPa. Endcaps were selected after shaping process by their mass and dimensions in order to avoid differences among the cavities.

Then one endcap for asymmetric cymbals or two endcaps for symmetric cymbal were bonded to a ceramic disk with a two-component epoxy (Eccobond) and cured under a small load of 136 kPa applied on the bonding area in a special die. The epoxy was spread just in the circumferential bonding area carefully keeping the cavity free from it.

The electrical impedance was measured as a function of the frequency with an impedance analyzer, Agilent 4294 using a frequency resolution of 0.1 kHz. To avoid clamping and suppression of the vibration a sample holder was designed that allowed holding the cymbals between two tips positioned in the bonding area.

The effective piezoelectric coefficient d_{33}^{eff} consists of the d_{33} of the PZT disk and the contribution of the disk's d_{31}, which is redirected by the cymbal endcaps.[7] It was measured with a Berlincourt Meter at a frequency of 100 Hz.

For the electromechanical characterization, the specimens were subjected to a compression loading test using a self-aligning jig on a Instron servohydraulic machine with a load cell of 1000 N, to which a electrometer (Keithley 6517A) has been incorporated with the aim to measure the generated electric charge.[8] The damage point was studied by the application of a force up to the break point.

3. Finite element analysis

The design and development stages of the PZT-Kovar composite transducer have been analyzed through a commercially available finite element analysis, FEA, software using the ATILA® code.

In this work it is assumed a base model consisted of PZT-5A of 1 mm thickness, 12.7 mm diameter, 0.25 mm thick Kovar endcaps with 0.25 mm cavity depth and 8.6 mm cavity diameter, and 0.04 mm thick epoxy bond. Mesh with axisymmetric quadrilateral-shaped elements of four nodal points was employed.

Whereas the vibration modes of the symmetric cymbals are previously stablished, the modes of asymmetric cymbals are not yet studied. Then, a modal analysis for resonant asymmetric cymbal modes was realized.

FEA ATILA® models were generated to analyse the frequency behaviour of cymbals with different bonding layer thickness and epoxy meniscus or lacks of adhesive (at the inner termination edge of the bonding layer). In order to simplify the calculations, the ATILA® models were developed for an asymmetric cymbal due to its unique cavity resonance mode.

Also, static analyses were attempted for the electromechanical characterization simulation. A static force was applied to an asymmetric cymbal and the resulting stress field studied.

The consistency of the FEA calculations and experimental results were established in previous studies,[5,9] indicating that ATILA® codes can be used to model the behaviour of the cymbal.

4. Result and discussion

4.1. Frequency behaviour of cymbals as a function of the bonding layer

Fig. 1 shows the impedance as a function of frequency for an asymmetric cymbal (a), and a symmetric cymbal (b). The symmetric cymbal spectra shows resonance peaks in the range from 20 to 32 kHz (A), from 65 to 88 kHz (C) and at 181 kHz (radial). A pure spectrum in region A is only found in 20% of the cymbals, the majority of the impedance spectra shows double peaks instead of single endcap resonance peak. The resonance peak A is the main vibration mode related to the endcap vibration and gives the frequency for resonant applications. The lack of symmetry in different endcap parameter like cavity height, cavity diameter, bonding defects and asymmetric deformations of the endcap contribute to the double peak characteristic.[10] In former studies[1] the resonance mode in region C was attributed to bonding problems, but following studies[5] demonstrated that this resonance peak was an harmonic vibration mode of the cavity. The peak at 181 kHz in the impedance spectra for symmetric cymbals corresponds to the radial mode of the PZT disk.

In asymmetric cymbals all endcap resonance peaks in region A are single peaks. In this case the unbonded side of the PZT disk is more free for radial displacement that the endcap bonded one, thus the system bends. In the case of symmetric cymbal both endcaps compensate and bending is prevented. Consequently the origin of the peaks which only appears for asymmetric cymbals, like peak at 47 kHz (B) and peak at 137 kHz (D), might be related to the bending motion.[11] The results of the FEA analysis are

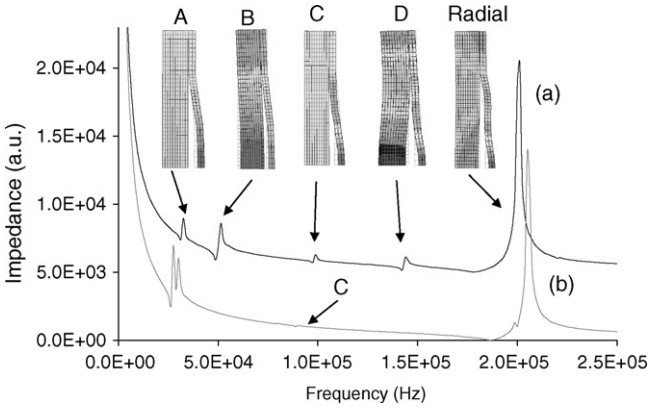

Fig. 1. Vibration modes of asymmetric (a) and symmetric cymbal (b).

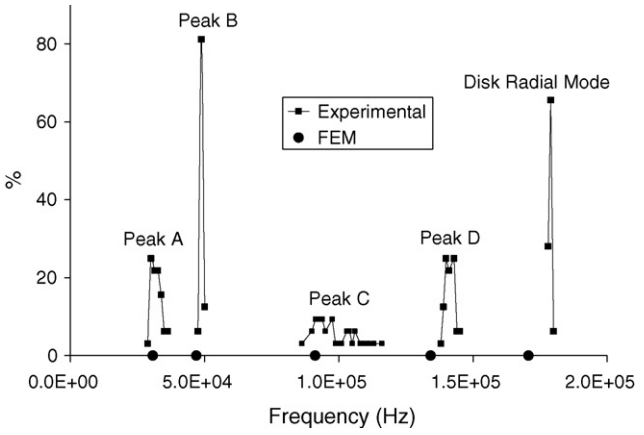

Fig. 2. Distribution of the resonant mode frequencies of an asymmetric cymbal.

shown in Fig. 1, and demonstrate that B and D are bending motion modes.

For statistical purposes a lot of 40 asymmetric cymbal was produced, and their resonance frequencies were measured. The resulting distribution is shown in Fig. 2. The cymbal devices show a resonance frequency distribution even with a careful selection of the dimension and weight of their components. The observation of cross sections of cymbals demonstrated the existence of inhomogeneities in bonding thickness generated by surface roughness as well the appearance of local meniscus and lacks of adhesive (Fig. 3). Then the presence of this inhomegeneties seems to be the origin of the resonant frequencies distribution. Because of the difficulty in the control of the width of the meniscus or the lack of adhesive and the thickness of the epoxy-bonding layer in laboratory conditions, FEA analysis was attempted. The frequency variation of the different resonant modes of asymmetric cymbal were analysed as a function of the bonding layer.

Fig. 4 shows the variation of the different resonance mode frequencies with the adhesive layer thickness calculated by FEA. The main cavity resonance mode (A) and its harmonic (C) are the most affected with the bonding layer thickness variation. Reductions up to 12% in the resonance frequency for the cavity

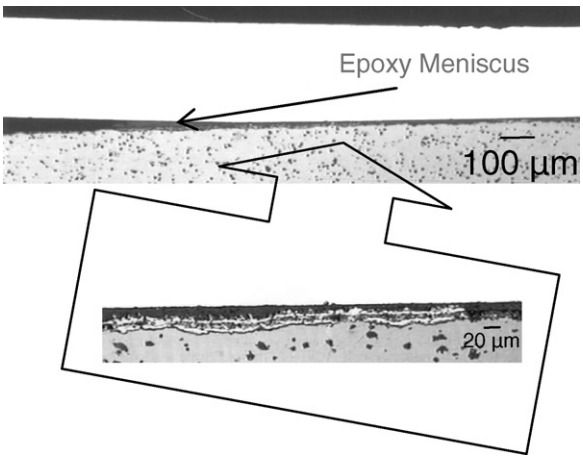

Fig. 3. Polished cross-section of the bonding layer of the cymbal. The inset shows a magnification of the bonding layer.

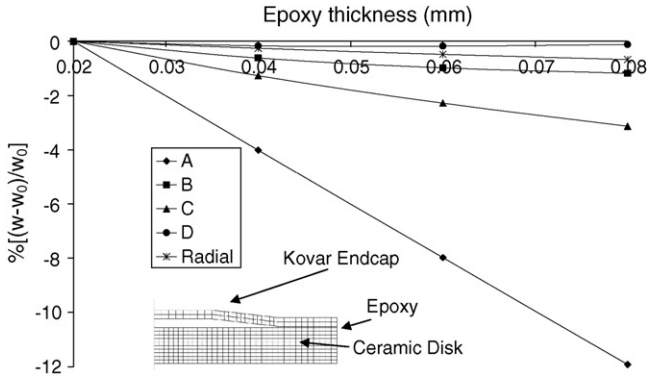

Fig. 4. Frequency variation in function of the bonding layer width.

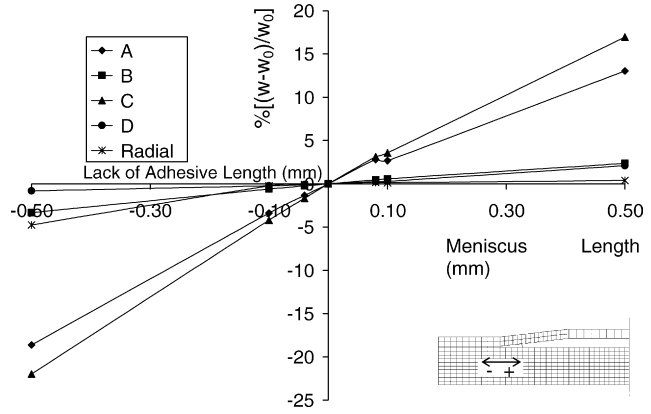

Fig. 5. Variation of the resonant frequency as a function of the meniscus length (positive) or lacks of adhesive (negative).

resonance mode could be reached by increasing four times the layer thickness.

The results of the FEA analysis of the resonance mode frequencies variation in function of the meniscus (positive values of the *x*-axis) or lack of adhesive (negative values of the *x*-axis) length are shown in Fig. 5. In this case the most affected mode is the harmonic cavity resonance mode, with variation in its frequency up to 20%. The fundamental cavity resonance mode is also largely affected. On the contrary the other resonance modes (B, D and radial) hardly are affected.

Table 1 compares the FEA analysis of the ratio stress/maximum displacement reduction of the at resonance frequency for the bonding layer variations, as well as other variables, like the stress concentration at the bonding layer at 100 Hz and maximum displacement of the cymbal at 100 Hz.

Firstly, a variation of the width of the meniscus was modelled, and the biggest reduction in the ratio stress/displacement, 23%, is obtained for a 0.5 mm meniscus epoxy width. This geometry

Table 1
Effect of the bonding layer variation

	Δ Stress/*d* at cavity resonance frequency (%)	Δ Stress at 100 Hz (%)	Δ*d* at 100 Hz (%)
Epoxy meniscus	−23	1.2	−24
Epoxy thickness	−37	1.5	−9

has serious disadvantages: the distortion of the cavity resonance mode and the decrease of the displacement (24% less at 100 Hz).

The effect in the stress concentration of a change in epoxy thickness was investigated. A reduction of the ratio stress/displacement of 37%, and a reduction of the displacement of 9% were obtained for an epoxy thickness of 0.1 mm width.

4.2. Electromechanical characterization

With the standard mechanical test the applied force versus displacement is recorded (Fig. 6a) but electrical information is lost. For example, the breaking point is not always revealed in this curve since the rupture was produced by the debonding of the endcap that remained in contact with the ceramic disk because of the applied force. Due to this, the generated charge versus applied force is required as a way to detect the point of debonding related to lack of continuity in the generated charge. The asymmetric cymbals were axially loaded in a universal mechanical test machine and the cycle monitored by an electrometer, and the generated charge versus applied force was represented (Fig. 6b).

The rupture was produced by the debonding of the endcap in a 67% of the samples, by cracking of the ceramic in a 20% and in a 13% the rupture does not occur. In this case the properties were degraded, then, a partially debonding of the endcap could be produced. The debonding or damage point is indicated by a leap in the charge versus force curve, since in this point the endcap and the ceramic loose the electrical contact for a while. This force is named here as "bond breaking force".

Physically, the slope of this curve is related with the effective piezoelectric coefficient of the cymbal, d_{33}^{eff}, due to differences between the area of charge collection and the area of force application. The behaviour must be similar but the magnitude required a correction factor. In former paper, the effective coefficient has been studied and calculated by using a mechanical approach.[7] Starting from the polarization vector due to the stress acting on the piezoelectric ceramic it is possible to calculate the effective piezoelectric coefficient for an asymmetric cymbal:

$$d_{33}^{\text{eff}} = -d_{31}\frac{r_t(r_t - r_1)}{t_h(t_c + t_m)} + d_{33} \quad (1)$$

where r_1 is the radius of the top part of the endcap cavity, r_t the radius of the bottom part of the cavity, t_h the height of the cavity, t_c the thickness of the ceramic disk, t_m is the thickness of the metal endcap.

According with this theoretical model, the d_{33}^{eff} might increase with decreasing cavity depth. The slope of the charge versus force curve increase until a maximum value, then decrease and finally remains constant. The behaviour could be attributed to the dimensional change of the cavity during the application of the force. The higher is the applied force, the smaller is the cavity depth due to the endcap deformation. The smaller the cavity depth, the higher the radial component of the stress induced in the ceramic disk. But, when the cavity depth decreases, the wall endcaps start to bend, and the effective force transfer from the endcap to the ceramic disk is reduced. This behaviour produces the existence of a maximum in the rate of the slope (the d_{33}^{eff} improvement). The applied force that produces this maximum in the slope variation could be associated with the blocking force of the cymbal[2] and it's named here "elastic endcap limit" because beyond this point the endcap start to have a permanent deformation (the cavity height deformation decreased a 22%, on average, after test). When the cavity is completely deformed, the slope remains constant up to the bonding layer failure.

It is possible to approach calculate d_{33}^{eff} from the slope of the charge generated versus applied force curve by multiply it by the ratio between the areas of force application and charge collection. At low applied force, that it is linear response, the resulted d_{33}^{eff} is (3200 ± 100) pC/N that are in good agreement with the Berlincourt Meter measurement of (3500 ± 650) pC/N because the cavity just starts to change its dimensions, and the geometries are comparables. For higher applied forces the d_{33}^{eff} increase up to (4122 ± 100) pC/N due to the cavity height decreasing. Beyond the elastic endcap limit, the slope became almost constant and d_{33}^{eff} is rather lower, (920 ± 60) pC/N, but still larger that (400 ± 10) pC/N of the ceramic disk. The endcap is still glued to the ceramic disk and part of the radial force is still transfer to the ceramic disk although the wall endcap are bended. After the bond breaking point, the approximated d_{33}^{eff} decrease up to (600 ± 50) pC/N. This value is rather bigger than the PZT disk one, the reason might be that the endcap clamps mechanically with the ceramic disk (joined by the friction and the force

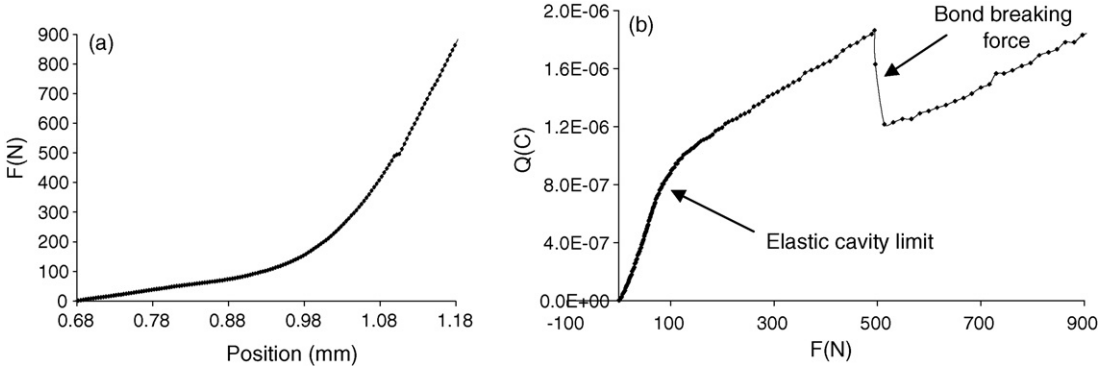

Fig. 6. Force in function of the position (a) and charge generated in function of the applied force (b).

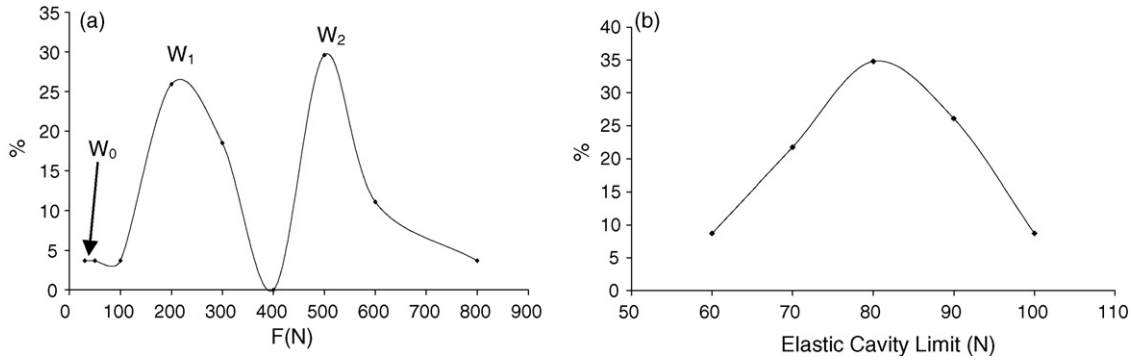

Fig. 7. Bond breaking force distribution (a) and elastic cavity limit distribution (b).

exerted), and transfer radial force to the ceramic disk in some extend.

Fig. 7a shows the bond breaking point distribution. Three different set of values are observed. The first group, denominate W_0, with rupture values under 100 N is related with serious defect in the bonding layer (Fig. 8a), which were previously detected by the impedance spectrum measurements. There are two other group, W_1 (lower breaking forces) and W_2 (larger breaking forces). A statistical test of independence, the Fisher's exact test,[12] was realised, and shows that W_0, W_1 and W_2 are statistically significantly different from a statistical point of view.

In order to understand the origin of the differences, the nature of debonding was studied. In 47% of the samples the bonding layer breaks by the complete adhesive separation of the ceramic disk. This adhesive failure can result from either inadequate surface treatment or material mismatch. Cohesive failure of the adhesive occurs when the load exceeds the adherent strength, and the bond fails within the adhesive itself, (20% of the samples). This cohesive failure is always to be desired. In 20% of the samples the ceramic disk was cracked. Also, in 13% of the cymbals the rupture doesn't occur. Theses percentages of adhesive or cohesive failure are the same in the two groups, W_1 and W_2 and in the whole set. Then the difference between W_1 and W_2 set of samples is not the nature of debonding.

With the aim of determinate the difference between W_1 and W_2, the breaking surfaces was observed with a magnifying glass. A bigger amount of defect as bubbles or lacks of adhesive were found in the W_1 set of samples (Fig. 8b) than in the W_2 set, then the difference between W_1 and W_2 set of samples is the larger presence of adhesive defect (as bubbles or lacks of adhesive). Due to this, a more reliable epoxy application, with a automatic dispensator for example, would reduce the number of defects and increase the W_2 set at the expense of W_1 set, and thus improving the bond breaking force. Even so, without the W_0 set of samples, the damage point is above the blocking force,[2] which is, for Kovar endcap, 65 N.

Fig. 7b shows the elastic endcap limit distribution. The elastic endcap limit seems not be related with the bonding layer or with the presence of defects. Then, the asymmetric cymbal devices can work up to 60 N without properties damage. The blocking forces previously reported, 65 N, are within the elastic endcap limit distribution. Then both magnitudes seems to be the same, but measured by different methods.

The main loading modes of bonded joints are: tensile or compressive loads imposed on adherends; shear stresses produced by out-of-plane tensile loads; cleavage loads produced by out-of-plane tensile loads acting on stiff and thick adherends at the ends of the joints; peel loads produced by out-of-plane loads acting on thin adherends. The aim of designing adhesive joints is to maintain the adhesive in a state of shear or compression because bonded joints are strongest under these loading conditions. Cleavage or peel forces should be avoided, or their effect minimised because concentrate the force in a bonding line in

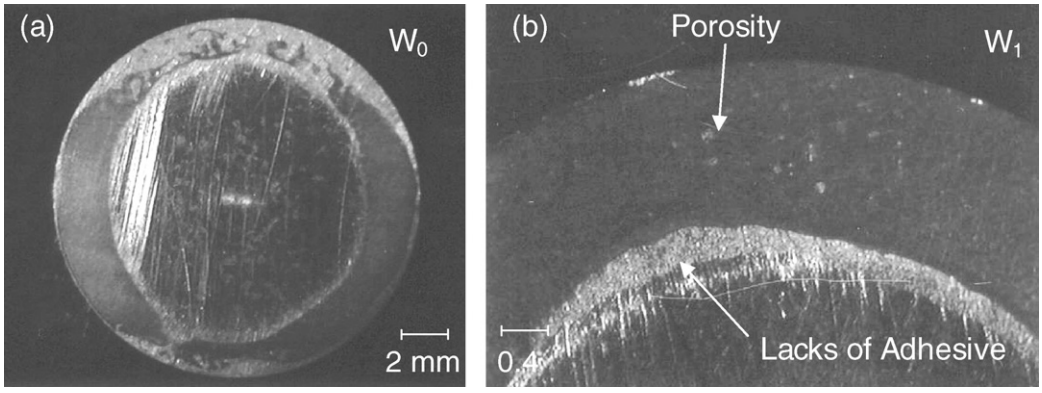

Fig. 8. Debonding endcap surface of W_0 (a) and W_1 (b) set of samples showing the adhesive defects.

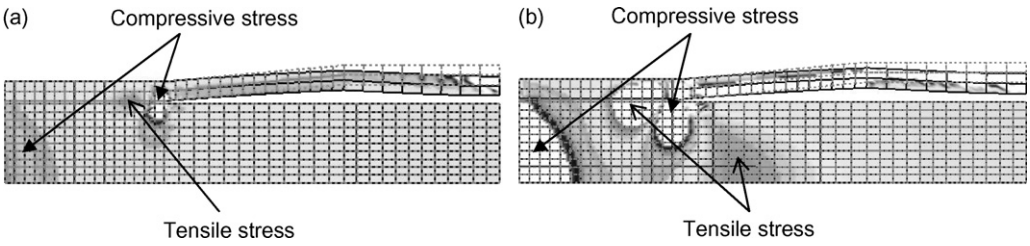

Fig. 9. Stress distribution on an asymmetric cymbal by FEM (a) and the same figure with the scale of the representation increased (b).

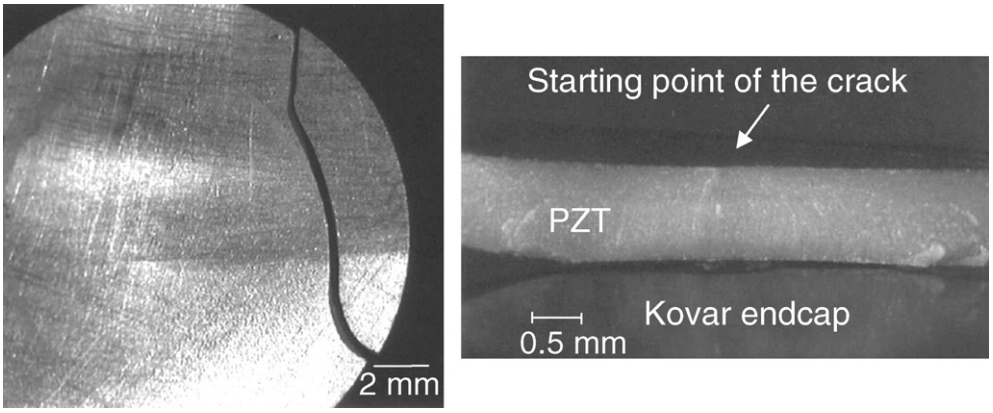

Fig. 10. Ceramic disk with a crack (left) and cross-section of the fracture surface (right).

spite of in the whole bonding surface. Tension forces easily could derivate in cleavage or peel forces. A static FEA of the electromechanical response test was developed with the aim to study the stress distribution. The result is shown in Fig. 9a. The largest stress concentration is observed at the inner termination edge of the bonding layer. This stress is compressive, but in the vicinity of this compressive stress there is a tensile stressed region. In this area the bonding layer is put to test by the worst loading mode, cleavage. Then, the presence of an adhesive defect initialises a crack which quickly grew under the stress producing the debonded of the cap. If the scale of the representation is increased (Fig. 9b) a tensile area in the ceramic is revealed. Ceramic materials have a reduced capability to support tensile efforts. If the crack surface of the ceramic is observed (Fig. 10), the crack line follows the inner termination of the bonding, starting in the opposite side of the endcap, just as the FEA analysis shows. The origin of this stress is in the bending motion of the devices that should be overcome by the presence of the other endcap in symmetric cymbals.

5. Conclusions

This work presents a statistical study of the different resonant modes of asymmetric cymbal. Using a FEA method these modes are identified and the experimental resonant frequency variation correlated with the bonding parameters as bonding layer width or the presence of epoxy meniscus and lacks of adhesive.

A rupture test has been developed for the study of the electromechanical behaviour of the cymbal piezocomposites. Using the generated charge versus applied force curves the reliability of these devices has been studied and the importance of the bonding layer determinate. A bonding layer with lower presence of defects will mean a larger break force.

Acknowledgements

This work has been financial supported by CICYT-DPI2002-0418-CO2-01. P. Ochoa was supported by a grant from FPI-CAM-FSE program.

References

1. Dogan, A., Flextensional 'moonie and cymbal' actuators, *Ph.D. Thesis*. The Pennsylvania State University, University Park, PA, 1994.
2. Fernandez, J. F., Dogan, A., Fielding, J. T., Uchino, K. and Newnham, R. E., Tailoring the performance of ceramic-metal piezocomposite actuators, cymbal. *Sens. Actuators A*, 1998, **65**, 228–237.
3. Pons, J. L., A comparative analysis of piezoelectric and magnetostrictive actuators in smart structures. *Bol. Soc. Esp. Ceram. V*, 2005, **44**, 146–154.
4. Zhang, J., Hladky-Hennion, A. C., Hughes, W. J. and Newnham, R. E., Modeling and underwater characterization of cymbal transducers and arrays. *IEEE Trans. UFFC*, 2001, **48**(2), 560–568.
5. Meyer, R. J., Hughes, W. J., Montgomery, T. C., Markley, D. C. and Newnham, R. E., Design of and fabrication Improvements to the cymbal transducer aided by finite element analysis. *J. Electroceram.*, 2002, **8**, 163–174.
6. Tressler, J. F., Alkoy, S. and Newnham, R. E., Piezoelectric sensors and sensor materials. *J. Electroceram.*, 1998, **2**, 257–272.
7. Ochoa, P., Villegas, M. and Fernández, J. F., Effective piezoelectric coefficient calculation of cymbal piezocomposite. *Ferroelectrics*, 2002, **273**, 315–320.
8. Cheng, B. L., Reece, M. J., Guiu, F. and Algueró, M., Fracture of PZT piezoelectric ceramics under compression-compression loading. *Scripta Mater.*, 2000, **42**, 353–357.

9. Ochoa, P., Pons, J. L., Villegas, M. and Fernández, J. F., Mechanical stress and electric potential in cymbal piezocomposites by FEA. *J. Eur. Ceram. Soc.*, 2005, **25**, 2457–2461.
10. Sugawara, Y., Onitsuka, K., Yhosikawa, S., Xu, Q., Newnham, R. E. and Uchino, K., Metal–ceramic composite actuators. *J. Am. Ceram. Soc.*, 1992, **75**, 996–999.
11. Ochoa, P., Villegas, M., Leidinger, P. and Fernandez, J. F., Vibration characteristic of cymbal type transducers. *Jpn. J. Appl. Phys.*, 2002, **41**, 7437–7440.
12. Bishop, Y. M., Fienberg, S. J. and Holland, P. W., *Discrete Multivariate Analysis: Theory and Practice*. The MIT Press, Cambridge, Massachusetts, 1980.